

Development of wind tunnel test model of mid-rise base-isolated building

Takeshi Ohkuma[†]

*Department of Architecture and Building Engineering, Kanagawa University,
3-27-1, Rokkakubashi, Yokohama, Kanagawa 221-8686, Japan*

Hachinori Yasui[‡] and Hisao Marukawa^{‡†}

*Urban Environment Research Center, Izumi Sohken Engineering Co., Ltd.,
51, Minami-sode, Sodegaura, Chiba 299-0268, Japan*

(Received October 15, 2003, Accepted March 23, 2004)

Abstract. This paper describes a method for developing a multi-degree-of freedom aero-elasto-plastic model of a base-isolated mid-rise building. The horizontal stiffness of isolators is modeled by several tension springs and the vertical support is performed by air pressure from a compressor. A lead damper and a steel damper are modeled by a U-shaped lead line and an aluminum line. With this model, the frequency ratio of torsional vibration to sway vibration, and plastic displacements of isolation materials can be changed easily when needed. The results of isolation material tests and free vibration tests show that this model provides the object performance. The peak displacement factors are about 4.5 regardless of wind speed in wind tunnel tests, but their gust response factor decreases with increment of wind speed.

Keywords: base-isolated building; wind tunnel test model; multi-degree-of-freedom model; elasto-plastic model.

1. Introduction

Concern and demand for the safety of buildings under strong earthquakes and function maintenance have risen since Southern Hyogo Prefecture Earthquake. An increasing number of base-isolated buildings have been built in Japan because they have excellent safety and quick function recovery after an earthquake. The base-isolation system was first mainly applied to low-rise and mid-rise RC building. However, it is now being applied from small-scale buildings like houses to the high-rise buildings over 60 m high. Base-isolated buildings tend to have a relatively long natural period.

This means that their natural frequencies are closer to the spectrum peak frequency of the wind force. Moreover, the ratio of the torsional natural frequency to the sway natural frequency is smaller than that of a conventional building. It is pointed out that torsional response results from a lack of

[†] Professor

[‡] Chief Research Engineer

^{‡†} Director

spatial correlation of wind pressure and contributes to the total response even for symmetrical buildings (Henderson, *et al.* 1990, Yasui, *et al.* 2002). In addition, it is feared that this will result in aerodynamic instabilities below the design wind speed, because the natural frequency decreases with plasticity of dampers, leading to increasing building displacements.

The behaviors of the buildings under wind forces have been estimated by several methods in many studies. Katagiri, *et al.* (2001) took account of motion-induced forces to estimate the response of a high-rise building. Marukawa, *et al.* (1996) developed a multi-degree-of-freedom aeroelastic model, and discussed the differences between the responses of the multi-degree-of freedom model and those of a stick model. Although this model is applicable in only the elastic range, it can clarify the complex vibration of the building, because each mass has three degrees of freedom. Tamura, *et al.* (2001) examined the across-wind direction response of a high-rise building using a degree-of-freedom stick model equipped with an elasto-plastic damper. This is pioneer research that deals with elasto-plastic behavior in a wind tunnel test. However, it is uncertain how to reproduce the objective building's response. In the research of Kawaguchi, *et al.* (1991), the responses of a building were analyzed step by step by a time-series analysis based on information obtained from on the dynamic force balance set model base, and the model is repeatedly moved up to the response by force. It is uncertain how the moving and stopping of the model influences the motion-induced wind forces.

The authors are researching the wind responses of base-isolated buildings. The main purpose is to develop an elasto-plastic model of a mid-rise base-isolated building for wind tunnel tests as a first step.

2. Outline of development process

The object building is the 23rd building of Kanagawa University, in which full-scale measurements of wind and earthquake responses are carried out. The seismic isolation layer of the building is installed between lower ground floor one and the second basement as shown in Fig. 1.

The base isolation layer of the object building is composed of 94 natural rubber bearings, 48 lead

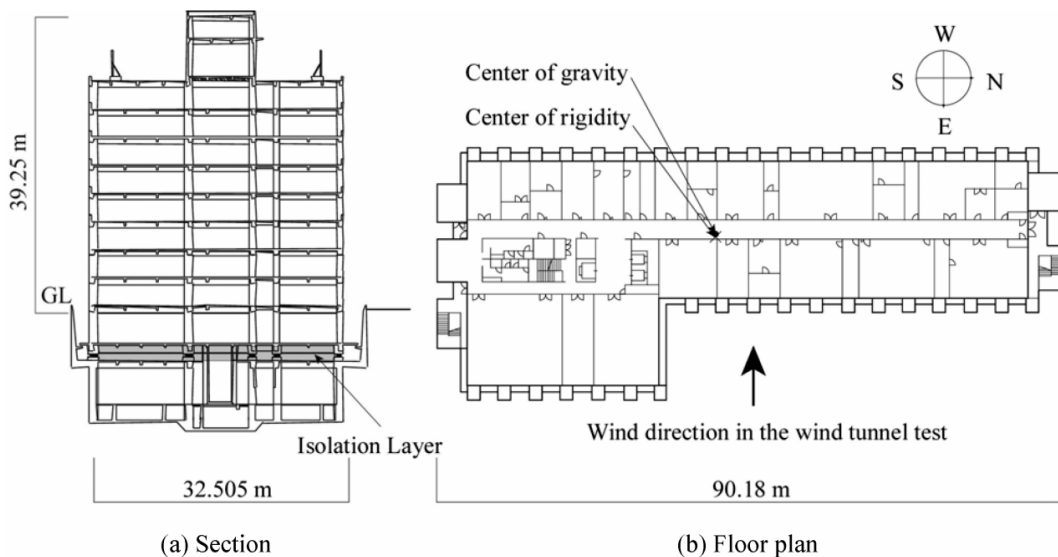


Fig. 1 Outline of objective building

Table 1 Characteristics of objective building and model

	Objective building	Model
Height (m)	39.3	0.197
Width (m)	90.2	0.451
Total weight (N)	2.91×10^8	36.4
Design wind speed (m/s)	39.7	5.0
Fundamental mode frequency in initial state (Hz)	0.72	18.1
Yield deflection of lead damper (mm)	8.30	0.04
Yield deflection of steel damper (mm)	32.5	0.16
Total yield force of lead dampers (N)	4.7×10^6	1.89
Total yield force of steel dampers (N)	5.1×10^6	2.05

dampers, and 20 steel dampers. It is confirmed that the rubber bearings show elastic behavior under an earthquake of the design velocity of 0.5 m/s. Their maximum face pressure under the earthquake is 1.81 kN/m^2 , and the minimum is 0.16 kN/m^2 . The lead damper is u-shaped, and the yield load is about 98 kN. The steel damper is formed from four looped bars, and the yield load is about 254 kN.

2.1. Outline of experiment model

The wind tunnel test model is scaled to 1/200 in consideration of the similarity law of air flow, the blockage rate of the wind tunnel and deformation at yield point of the seismic isolation material. The experimental wind speed corresponding to the design wind speed (39.7 m/s at building high) is set to 5 m/s as shown in Table 1. In this case, the fundamental mode frequency of the model corresponding to that of the objective building (0.72 Hz) at the design wind speed is set to 18.1 Hz.

The model has two lumped masses and a base isolation layer, as shown in Fig. 2, so it represents 6 degrees of freedom. The stiffness above the seismic isolation layer is modeled by four steel columns that have similar stiffness to the objective building. The maximum deflection of the seismic isolation layer of the model is set to 1 mm. The outer part of the model that corresponds to the external wall and the roof was covered with balsawood of 1 mm thickness.

2.2. Experimental model of isolator

The isolators installed in the object building show elastic behavior under an earthquake of the design velocity of 0.5 m/s. The maximum deformation is about 0.3 m under such an earthquake. The isolator model was required to show elastic behavior in the experiment. The following ideas were examined for the isolator model.

First, it was tried to model the stiffness of the isolators, including the stiffness above the seismic isolation layer, with steel columns. Results of trial calculations showed very slender columns. Because they would bend easily in production and experimentation, this idea was not adopted.

Second, the vertical stiffness and horizontal stiffness components were made separately, i.e. the horizontal stiffness was modeled by a spring and vertical support was modeled by ball bearings. However, the friction force of the ball bearings was so unexpectedly large that the model did not operate smoothly. The following was adopted in an experimental model of an isolator.

As shown in Fig. 2, the horizontal elastic stiffness of the isolator was modeled by eight cold-coiled tension springs. The positions of the springs were arranged so that the torsional stiffness of

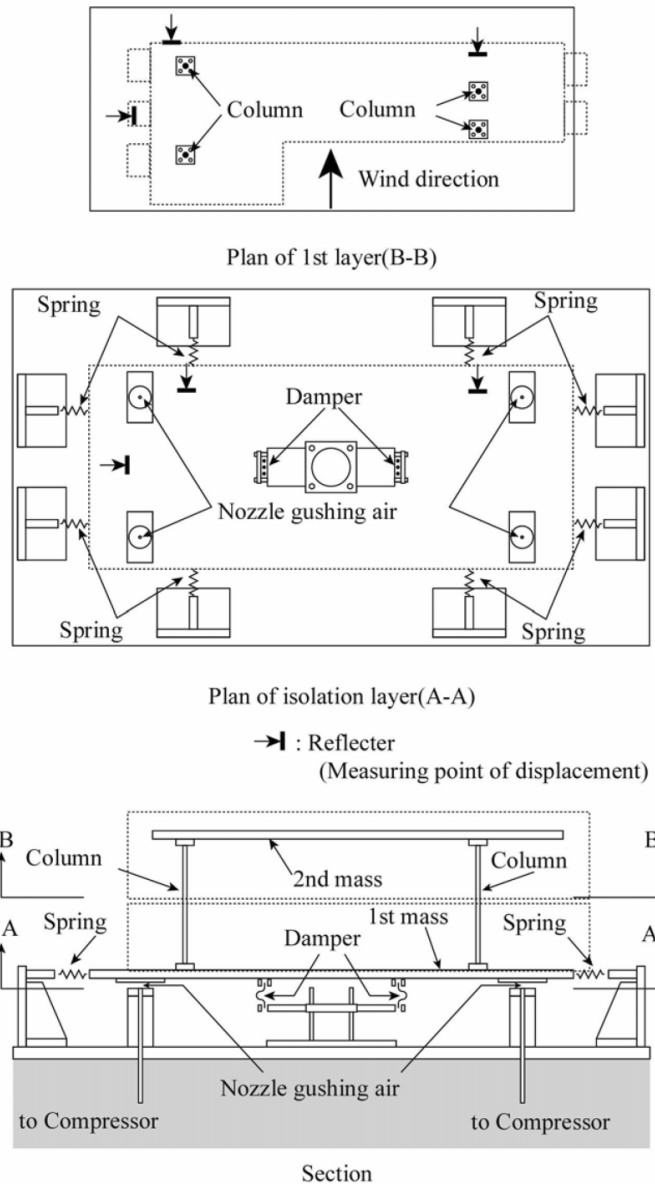


Fig. 2 Outline of wind tunnel test model

the model was similar to that of the object building. The vertical force, including the mass of the model, was supported by air pressure supplied by an air compressor. The damping ratio of the model without the damper was 0.2% or less.

2.3. Experimental model of damper

The yield deformations of the lead damper and the steel damper in the objective building were 8.3 mm and 32.5 mm. These correspond to 0.04 mm and 0.16 mm in the model, as shown in Table 1.

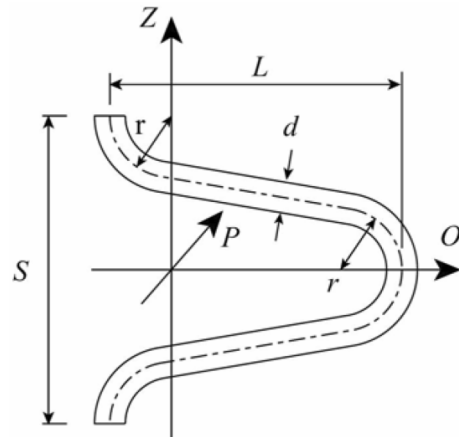


Fig. 3 Shape of experimental model of damper

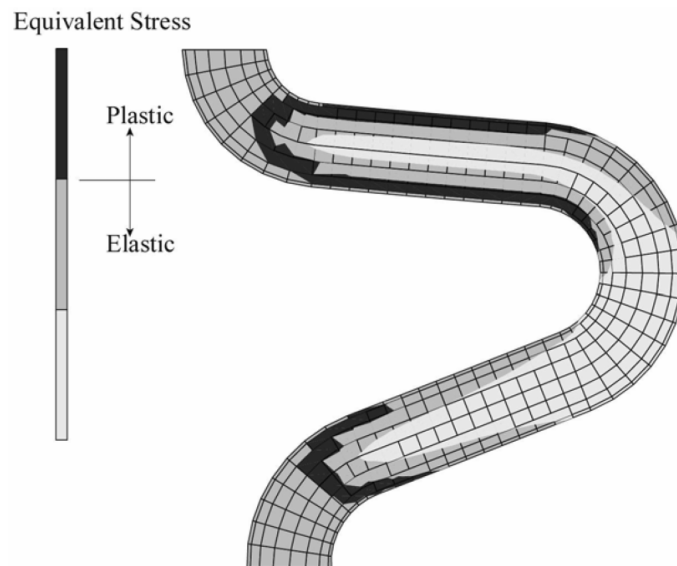


Fig. 4 Result of finite element analysis of lead damper model

Four or more materials have to be installed in the model in order to confirm the similarity of the torsional stiffness. It is necessary to adjust the length of a damper to 10 mm or less and its diameter to 1 mm or less if straight steel line is used. The following means were considered in producing the damper.

The damper has to operate to 10% as the maximum deflection angle, so geometrical nonlinearity cannot be disregarded. When the horizontal transformation increases, the axial tension force comprises the majority of the horizontal resistance force when using straight materials. As a result, the damper doesn't become plastic at the target yield load. Thus, the damper material was bent in one direction as shown as Fig. 3.

To determine the damper's shape so that its elastic stiffness and the yield deformation became similar to that of the dampers of the object building, a finite element analyses was carried out. The

parameters in the analyses were d , S and L , as shown in Fig. 3. The similarity of the stiffness after the damper became plastic is neglected.

Fig. 4 shows the equivalent stress distribution of a lead damper model obtained from finite element analysis. It is clear that a plastic region occurs at the edge of the damper.

The lead damper was modeled by a U-shaped lead line with $d=0.65$ mm, $S=4$ mm and $L=3$ mm, and the steel damper was modeled by a U-shaped aluminum line with $d=0.5$ mm, $S=7$ mm and $L=3$ mm.

Both ends of the damper were inserted into a square steel pipe filled with putty and fixed by the putty's hardening.

In general, because the aluminum line was cold-rolled out, its yield stress was 200-300 N/mm², which was higher than the target value. They were therefore annealed at 250°C in an electric furnace before and after bending to adjust the yield stress to the target one. The in-furnace temperature was measured with a thermo sensor (Anritsu, 1-K-J1M1-1000).

3. Basic performance of experimental model

3.1. Cyclic loading test of damper for model

The characteristic of the damper for the model was examined using a loading test device with a built-in load cell of 5.88 N capacity (MINEBEA, CB17-600G-11). Displacement was measured by the laser displacement sensor (Keyence, LB-080) installed in the device.

Figs. 5 and 6 show the results of the cyclic loading examination of the damper models. O-direction is in-plane of the U-shaped damper, and P-direction is out-of-plane, as shown in Fig. 3.

The hysteresis curves of the damper for both directions were the same shape regardless of the loading cycles. The elastic stiffness of both dampers corresponded to the target. The yield load and deflection of the steel damper model closely corresponded to the targets. The yield load of the lead damper model was a little higher than the target in the O-direction. This difference can be decreased by installing the two dampers orthogonally as a couple.

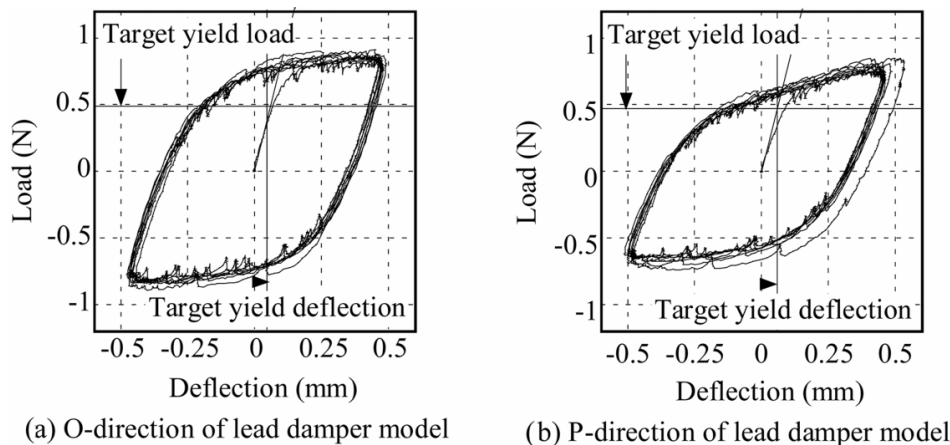


Fig. 5 Cyclic loading test of lead damper model

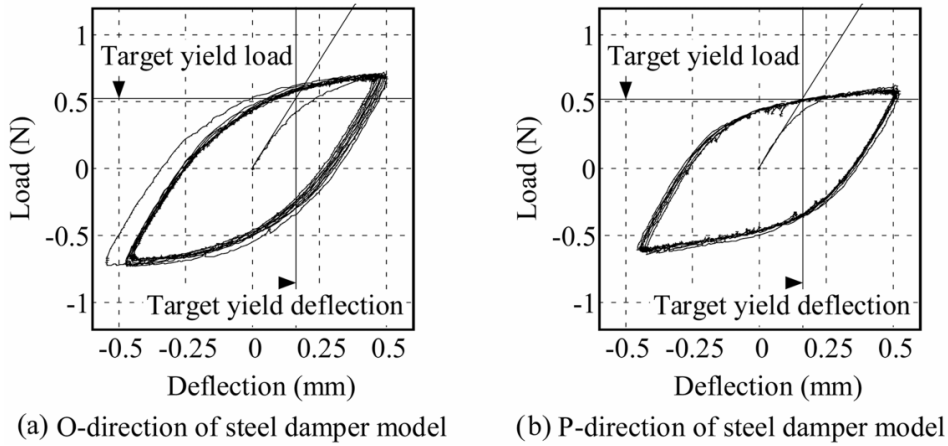


Fig. 6 Cyclic loading test of steel damper model

3.2. Free vibration test

The free vibration tests with various initial displacements were carried out before the wind tunnel tests. Fig. 7 shows the results of the free vibration test.

The damper model was elastic when the displacement of the seismic isolation layer was 0.03 mm (refer to Figs. 5 and 6). The natural frequency obtained from the free vibration tests was

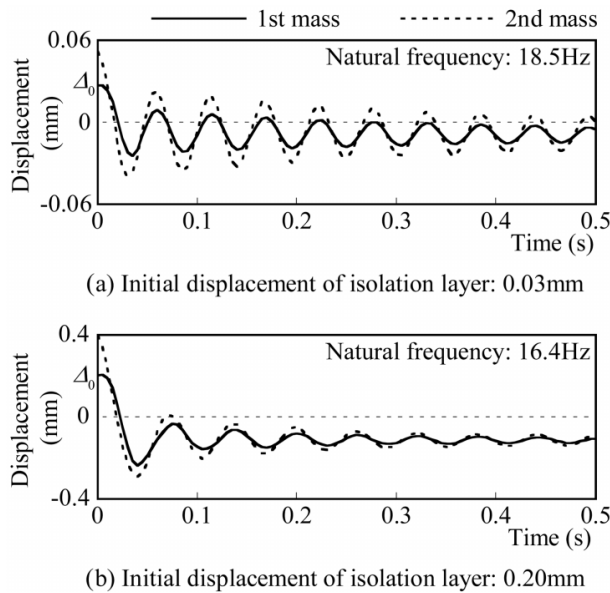


Fig. 7 Results of free vibration test

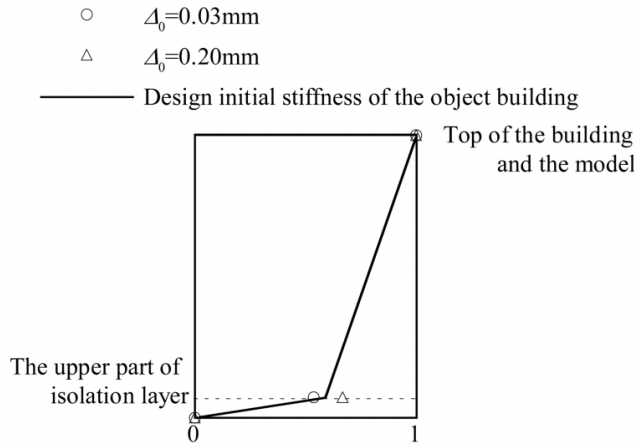
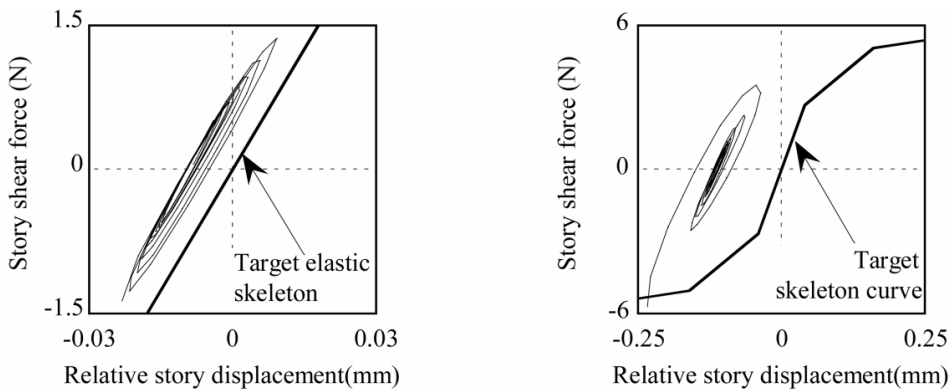


Fig. 8 Vibration mode of the model



(a) Initial displacement of isolation layer: 0.03mm (b) Initial displacement of isolation layer: 0.20mm

Fig. 9 Restoring force characteristics of isolation layer of model

18.5 Hz, which corresponds to the target of 18.1 Hz (refer to Table 1). The damping ratio calculated by the logarithmic decrement was 8% in the first half cycle and about 1% after that. The natural vibration mode corresponded closely to the target, although it is not shown in a figure.

The dampers were beyond the yield points when the displacement of the seismic isolation layer was 0.20 mm. The natural frequency obtained from the test was 16.4 Hz. The natural frequencies increased with decrement of the displacement. The damping ratio calculated by the logarithmic decrement was 14% in the first half cycle and about 2% after that.

Fig. 8 shows vibration modes of the model and the object building obtained from free vibration tests. The positions in which the amplitude of the mode is considered are both the top and the upper part of the base isolation layer. The vibration mode for the initial displacement of the isolation layer

corresponds to the mode assumed by the design. The ratio of the base isolation layer deformation to the model top deformation increases as the initial displacement increases. This causes plasticity in the base isolation layer.

Fig. 9 shows the relationship between the story shear force and the displacement of the isolation layer. The inertia force of each mass was calculated by multiplying the mass by the time-series acceleration that was obtained by differentiating the time-series displacement. The total of the inertial force was evaluated as the story-shearing force of the isolation layer. The model's elastic stiffness corresponds to the target elastic skeleton.

These results prove that the developed models exactly simulate the target building with a seismic isolation layer.

4. Wind tunnel test

4.1. Outline

The experimental direction is normal to the long side, as shown in Fig. 1. The mean wind speed at the model height was changed from 3.6 m/s to 13.5 m/s at about 0.5 m/s intervals. The response displacement was measured for 60 seconds at a sampling frequency of 200 Hz with the laser displacement sensor (Keyence, LK-030, LB-080 and LK-500) at each wind speed. The displacements were measured at the positions shown in Fig. 2.

4.2. Experimental results and discussions

Fig. 10 shows the relation between the mean wind speed at the model height and the response.

The mean displacement increased in proportion to the 2.8th power. This is greater than that for a conventional usual building because the dampers showed plastic behavior. However, the power of the standard deviation (S.D.) was 2.5, which is smaller than that of mean displacement.

The peak factor (P.F.) of the response displacement was about 4.5 regardless of the mean wind

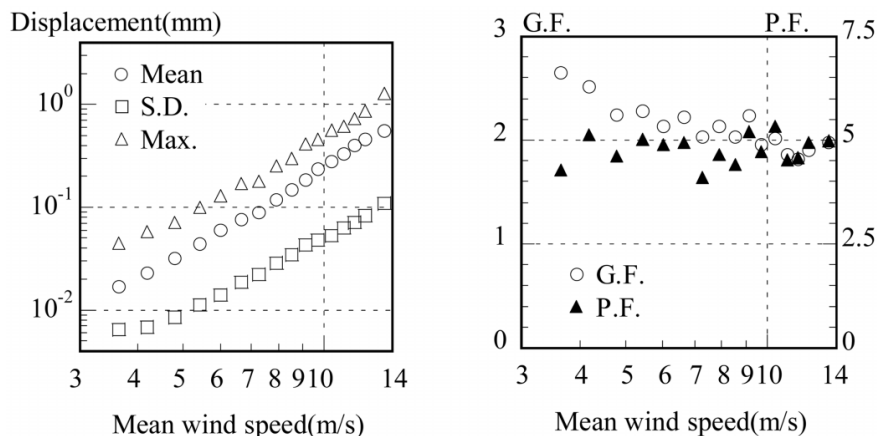


Fig. 10 Relation between wind speed and along-wind displacement at the model height

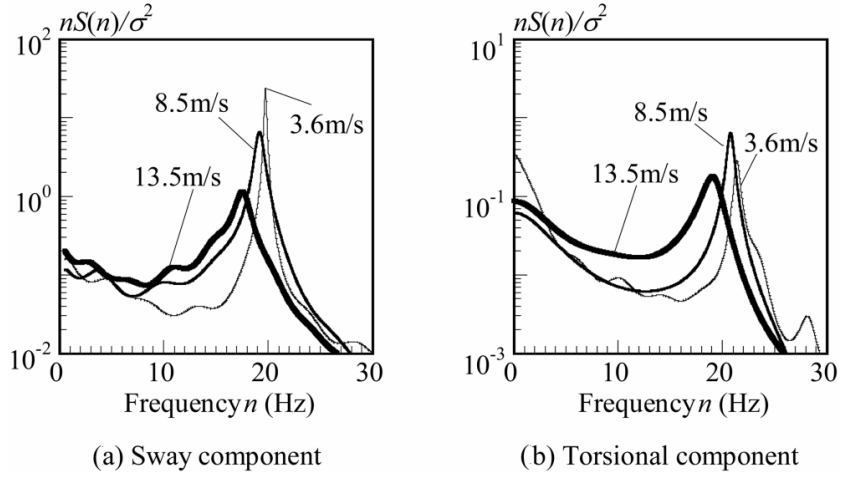


Fig. 11 Power spectrum densities of displacements

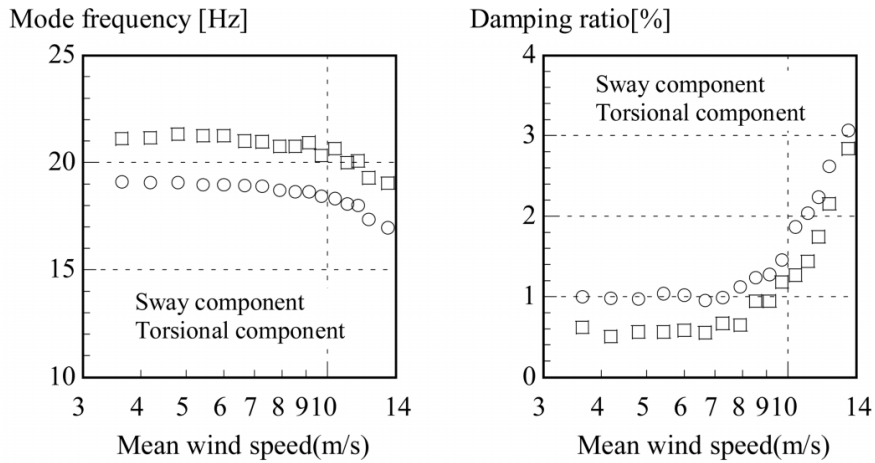


Fig. 12 Relation between wind speed and mode frequency and damping ratio

speed. This large peak factor is recognized in the full-scale observation [2]. The gust factor (G.F.) decreased as the wind speed increased, and reached 2 at 10 m/s.

Fig. 11 shows the power spectral densities of the response displacement in the second mass during 3.6 m/s, 8.5 m/s, and 13.5 m/s mean wind speeds at the model height. A mean wind speed of 3.6 m/s corresponds to the wind speed where the dampers behaved elastically, 8.5 m/s corresponds to the wind speed where the lead dampers reached the plastic region, and all of dampers became completely plastic for the mean wind speed of 13.5 m/s. The spectrum peak moved to the lower frequency side and the spectrum band became wider as the wind speed increased.

Fig. 12 shows the relation between the mean wind speed at the model height and the mode

frequency or damping ratio. Mode frequency and damping ratio are computed from power spectrum density. Both natural frequencies and damping factors are constant when the mean wind velocity is 8 m/s or less. When the mean wind velocity exceeds 8 m/s, the natural frequency decreases and the damping ratio increases. This is because some lead dampers reached the plastic region at 8.5 m/s. The damping ratio in the wind response test is smaller than that in the free vibration test. This is because there is oscillation only on one side in the wind response test.

5. Conclusions

An elasto-plastic model of a mid-rise base-isolated building for wind tunnel tests was developed and the basic performance and its response characteristics were confirmed. The following findings were obtained.

- (1) The elastic stiffness of the damper models corresponded to the target value. The yield load of the steel damper model corresponded to the target, but that of the lead damper model was a little higher. The hysteresis curves of the damper for both directions had the same shape regardless of the loading cycles.
- (2) The free vibration experiments on the model yielded a fundamental mode corresponding to the target one.
- (3) It was confirmed that the yield load of the aluminum damper could be adjusted by annealing.

Therefore, it was confirmed that the developed model exactly simulates the target building with a seismic isolation layer.

Moreover, the following findings were obtained concerning the wind response properties.

- (1) The mean displacement increased in proportion to the 2.8th power. This is greater than that of a conventional building, because the dampers showed plastic behavior. However, the power of the standard deviation was 2.5, which is smaller than that of the mean displacement.
- (2) The peak factor of the response displacement was about 4.5 regardless of the mean wind speed.
- (3) The gust response factor was 1.8-2.8 and decreased as the wind speed increased.

Acknowledgements

The authors wish to extend their thanks for supporting by the Academic Research Frontier Promotion of MEXT (Ministry of Education, Culture, Sports, Science and Technology), and the Industrial-government-academic Joint Project of Kanagawa University "Typhoon and Earthquake-induced Disaster Control and Mitigation, Project leader: Takeshi Ohkuma".

References

- Henderson, P. and Novak, M. (1990), "Wind effects on base isolated buildings", *J. Wind Eng. Ind. Aerodyn.*, **36**, 559-569.
- Katagiri, J., Ohkuma, T. and Marukawa, H. (2001), "Motion-induced wind forces acting on rectangular high-rise

- buildings with side ratio of 2", *J. Wind Eng. Ind. Aerodyn.*, **89**, 1421-1432.
- Kawaguchi, A., Maruta, E. and Kanda, M. (1999), "Hybrid vibration system for evaluation of wind forces on structures", *Proc. 10th Int. Conf. on Wind Engineering*, Copenhagen, pp. 445-460.
- Marukawa, H., Katagiri, J., Katsumura, A. and Fujii, K. (1996), "Development of multi-degree-of-freedom aeroelastic model and evaluation of wind response of a high-rise building", *J. Structural and Construction Engineering* (Transactions of AIJ), **484**, 39-48, in Japanese.
- Tamura, T., Okada, R. and Wada, A. (2001), "Wind tunnel test of across wind oscillations for high-rise building model with hysteretic damper", *J. Structural and Construction Engineering* (Transactions of AIJ), **547**, 51-58, in Japanese.
- Yasui, H., Ohkuma, T., Koga, S. and Shimomura, S. (2002), "Full-scale measurement of wind-induced response of a base-isolated mid-rise building", *Proc. 17th National Symposium on Wind Engineering*, Tokyo, pp. 445-450, in Japanese.

CC